

## COMPUTER SIMULATION OF DISLOCATION PATTERN FORMATION

N.M. Ghoniem and R. Amodeo

Mechanical, Aerospace and Nuclear Engineering Department  
University of California, Los Angeles  
Los Angeles, CA 90024, USA

### ABSTRACT

A computer simulation of the behavior of individual dislocations is presented. The equations of motion of individual dislocations are simultaneously solved using extensions of dynamical particle simulation methods [i.e., molecular dynamics, Langevin dynamics, and the Monte Carlo methods]. The evolution of one- and two-dimensional (2-D) patterns is illustrated by computer simulation of dislocation dynamics. In 1-D patterns, criteria for accurate numerical simulation of dislocation pileup evolution are established. The potential for using specialized numerical and computational techniques to reduce the demands on existing computers is discussed.

### 1. INTRODUCTION

Recent advances have been made in the field of computational statistical mechanics and the non-linear science of pattern formation. The advent of high-speed supercomputers and special architectures has allowed simulation of the time evolution of larger numbers of particles in molecular systems, both gaseous and liquid [1]. In the field of non-linear science, the last decade has produced a wealth of new concepts and ideas which contributed to an almost new picture of the nature of science [2]. In this paper, we attempt to show that the marriage of these two fields offers an exciting approach to the simulation of dislocation dynamics. This approach is of great significance to understanding the origins of plasticity, creep, fatigue, and fracture of solids.

Dislocation climb and glide mobilities are determined by a combination of mechanisms under the influence of high temperature, stress, and irradiation. It is experimentally observed that at critical values of these conditions, regular 1-, 2-, and 3-D patterns of dislocations form within the material [3]. These patterns are linear slip bands [4], hexagonal [5], and dislocation rods [6] in one, two, and three dimensions, respectively. These dislocation structures play a significant role in dislocation production and recovery processes, which control the rate of high-temperature deformation. The dislocation cell structure, which will be discussed in this paper, can be described as a 2-D honeycomb-like configuration in which there are regions of high dislocation density (cell walls) and low dislocation density (the region between the walls).

The earliest significant theoretical model of dislocation cells was developed by Holt [7]. His analysis, which is an extension of linear spinodal decomposition theory, attributed the onset of the spatial instability to a global minimization of the elastic free energy. Since Holt's original work, several rate theories have been developed which demonstrate specific aspects of dislocation dynamics in cells (e.g., Argon and Takeuchi [8] and Sandstrom [9]). More recently, Prigogine's stability analysis of chemical kinetics [2] has been extended by Walgraef and Aifantis [3,10], Schiller and Walgraef [11], and Murphy [12] to analyze dislocation structures. They consider two types of dislocations, mobile and immobile, in a set of reaction-diffusion equations. Their work shows that the competition between diffusive mobilities and cubic nonlinearities for the pinning of mobile dislocations by immobile dipoles leads to stable periodic dislocation structures.

Particle simulation has been a major tool in computational physics [13]. When the interaction force between particles is long range, such as the force due to a charged particle (Coulomb field), the influence of all other particles must be computed at every timestep. This leads to algorithms with  $O(n^2)$  complexity, where  $n$  denotes the number of particles. Dislocations, which are essentially 2-D discontinuities in the atomic stacking, will be regarded as macroscopic point particles. Theory of elasticity is used to determine the long-range interaction forces, and short-range interactions are approximated as events or processes. A basic feature in dislocation dynamics (DD) is that dislocations are limited to motion along the plane of discontinuity (climb) and perpendicular to the plane of discontinuity (glide). This paper presents a model for the numerical simulation of dislocation dynamics within the framework of particle methods. The model is applied to the evolution of 1-D pileup patterns and to 2-D dislocation interactions. Methods to overcome computational limitations, and the effects of various dislocation processes on pattern formation will be discussed.

## 2. THEORETICAL MODEL

Two categories of computational methods have been applied to the simulation of atomic and molecular systems. In the first category a non-dynamical approach, the Monte Carlo (MC) method, is used to obtain information on ensemble averages by using random sampling techniques. In contrast, dynamical methods yield the trajectories of a number of interacting physical entities. The term molecular dynamics (MD) has been used to describe the early versions of such calculations. In 1980, Andersen [14] proposed a mixed MC/MD algorithm for isothermal simulations where stochastic collisions are treated in accord with the MC technique. In the following, we present a DD model, which is based on particle simulation ideas used in molecular systems.

In our model, we represent the grain by a 2-D plane enclosed by grain boundaries. Edge-type dislocations are studied and they are assumed to be straight, parallel, and perpendicular to the observation plane. Dislocations can glide only along glide directions, and they can also climb normal to glide directions. The Peach-Koehler equation for the force per unit length,  $F/L$ , acting normal to the dislocation line, is given by [15]:

$$\vec{F}/L = (\vec{b} \cdot \bar{\Sigma}') \times \vec{\xi} \quad , \quad (1)$$

where  $\bar{\Sigma}' =$  stress dyadic (tensor) ,

$$\begin{aligned} &= \sigma_{11}^{\hat{i}\hat{i}} + \sigma_{12}^{\hat{i}\hat{j}} + \sigma_{13}^{\hat{i}\hat{k}} + \sigma_{21}^{\hat{j}\hat{i}} + \sigma_{22}^{\hat{j}\hat{j}} + \sigma_{23}^{\hat{j}\hat{k}} \\ &+ \sigma_{31}^{\hat{k}\hat{i}} + \sigma_{32}^{\hat{k}\hat{j}} + \sigma_{33}^{\hat{k}\hat{k}} \quad , \quad (2) \end{aligned}$$

and  $\vec{\xi} =$  unit tangent vector to the dislocation line .

Figure 1 shows a test edge dislocation,  $t$ , and a reference dislocation,  $r$ , in a global coordinate system. The position of the test dislocation is given by the vector  $\vec{R}_t$ , the position of the reference dislocation is given by the vector  $\vec{R}_r$ , and their connecting vector angle in the global system is  $\delta$ . The Burgers vectors of the two dislocations are defined by  $\alpha_t$  (the test dislocation rotation angle) and  $\alpha_r$  (the reference dislocation rotation angle). The parameters  $\vec{R}_t$ ,  $\vec{R}_r$ ,  $\delta$ ,  $\alpha_r$ , and  $\alpha_t$  completely define all degrees of freedom of the two dislocations. For example, in the test dislocation system, the connecting vector angle is

$$\theta = \delta - \alpha_t \quad , \quad (3)$$

and the relative rotation angle of the reference dislocation Burgers vector is

$$\gamma = (\alpha_r - \theta) - \alpha_t \quad , \quad (4)$$

The stress field produced by the test dislocation, in its own cylindrical reference system, is described by the 2-D tensor

$$\bar{\Sigma} = \begin{pmatrix} \sigma_{rr} & \sigma_{r\theta} \\ \sigma_{\theta r} & \sigma_{\theta\theta} \end{pmatrix} = f(R) \begin{pmatrix} -\sin\theta & \cos\theta \\ \cos\theta & -\sin\theta \end{pmatrix} \quad , \quad (5)$$

where

$$f(R) = \frac{\mu |\vec{b}_t|}{2\pi(1-\nu)} \cdot \frac{1}{R} \quad , \quad (6)$$

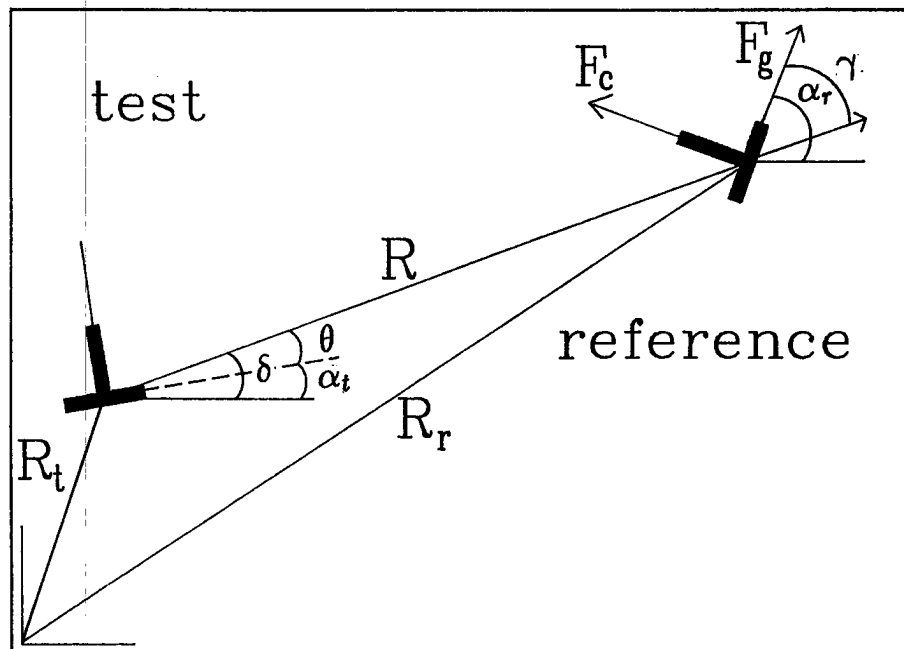


Figure 1. Coordinate system for two interacting dislocations.

and  $\mu$  is the shear modulus,  $\vec{b}_t$  the reference dislocation Burgers vector,  $\nu$  is Poisson's ratio, and  $R$  the inter-dislocation distance. The force on the reference dislocation is obtained by applying the Peach-Koehler equation (1), together with equation (5), with  $\vec{\xi}_r = \vec{\xi}_t = \vec{k}$ . However, in order to obtain the climb and glide components of the force, we must describe the stress field in the Cartesian global coordinate system. The stress transformation tensor,  $\bar{\bar{T}}$ , is given by

$$\bar{\bar{T}} = \begin{pmatrix} \cos\gamma & \sin\gamma \\ -\sin\gamma & \cos\gamma \end{pmatrix}, \quad (7)$$

and the stress dyadic,  $\bar{\bar{\Sigma}}'$ , in the global coordinate system is given by

$$\begin{aligned} \bar{\bar{\Sigma}}' &= \bar{\bar{T}} \cdot \bar{\bar{T}} \cdot \bar{\bar{\Sigma}} \\ &= f(R) \begin{pmatrix} (-\sin\theta + \sin 2\gamma \cos\theta) & (\cos\theta \cos 2\gamma) \\ (\cos\theta \cos 2\gamma) & -(\sin\theta + \sin 2\gamma \cos\theta) \end{pmatrix}. \end{aligned} \quad (8)$$

Finally, the glide and climb forces on the reference dislocation are given by

$$\frac{F_g}{L} = \frac{\mu |\vec{b}_t| |\vec{b}_r|}{2\pi(1-\nu)} \left( \frac{\cos\theta \cos 2\gamma}{R} \right), \quad (9)$$

$$\frac{F_c}{L} = \frac{\mu |\vec{b}_t| |\vec{b}_r|}{2\pi(1-\nu)} \left( \frac{\sin\theta - \sin 2\gamma \cos\theta}{R} \right), \quad (10)$$

For the case  $\gamma + \theta = \alpha_r - \alpha_t = 0$ , expressions (9) and (10) are identical to well known equations for climb and glide forces of two parallel dislocations. The total glide and climb forces on the reference dislocation are obtained by a linear scalar summation of each component over the total number of dislocations.

It is found experimentally that the internal glide and climb velocities of dislocations are simply proportional to the respective force [16-18]. The proportionality constants are termed mobilities, which are dependent on temperature, jog concentration, stacking-fault energy, and irradiation conditions. The addition of an external shear stress to the system results in another added component of the glide velocity. Once the components of velocities are calculated in the reference dislocation system, they can easily be converted to the global coordinate system. An explicit integration over a timestep,  $\Delta t$ , determines the global coordinates of the reference dislocation. This procedure has to be repeated for all interacting dislocations in order to describe the evolution of the set of dislocations.

Short-range forces are also considered in addition to the elastic long-range inter-dislocation forces. These forces result in higher order non-linear reactions and the onset of dislocation clustering. The following dislocation reactions are accounted for during the simulation: (1) Interaction of dislocations with grain boundaries; (2) Immobilization reactions due to equilibrium long-range elastic fields, precipitates, or attractive junction formation; (3) Dislocation annihilation; (4) Dislocation dipole formation.

Production of new dislocations by the Frank-Reed or Bardeen-Herring mechanisms will be included in future simulations. It is to be emphasized that while short-range interaction forces are treated at a basic level, the main features of dislocation dynamics are still revealed by the simulations. Also, higher order non-linear reactions, which include dislocation clustering, are treated as natural consequences of the dynamic system evolution.

Dislocations coming in contact with grain boundaries will either stop at the boundary, where pileups can occur, or are absorbed into or transmitted through the boundary. The rate of absorption is limited by the climb of dislocations into the boundary. Dislocation absorption, or "spreading," results in the disappearance of long-range stress fields associated with dislocations. This process tends to occur in low stacking-fault energy materials, in which recrystallization is more likely to occur than dynamic recovery. Therefore, it appears that absorption is not normally characteristic of materials in which dislocation cells form. Dislocations are more likely to be trapped at grain boundaries in materials with high stacking-fault energies. Dislocations become unable to re-form the grain boundary front and initiate re-crystallization. In these materials, subgrains are more likely to form, accounting for the recovery process which is necessary to relieve the high strains produced in the grain. In the present simulations, we consider the grain boundary force as a result of the misorientation of two adjoining grains. This misorientation produces a stress  $P$  at a point of distance  $x$  from the grain boundary on the order [19]

$$P = 2\mu\psi\eta e^{-\eta} \quad , \quad (11)$$

where

$\psi$  = angle of grain misorientation,

$\eta = 2\pi\psi|x|/b$ ,

$b$  = normalized distance, Burgers vector.

Annihilation events are registered if dislocations of opposite sign come within a critical inter-dislocation distance. The value of this distance is on the order of 1.6 nm [20], which is about an order of magnitude less than the average distance of dislocations within the cell boundary. If the two dislocations come within a distance that is slightly larger than this critical value, a dislocation dipole is formed. Attractive dislocation junctions are allowed to form when the Burgers vectors of the two dislocations are not of the exact opposite sign. Finally, a dislocation is immobilized in one of the following cases: (1) If it undergoes 30 to 40 position oscillations due to the long-range stress field; (2) If it encounters an obstacle (i.e., a junction, dipole, or a group of dislocations).

### 3. ONE-DIMENSIONAL SIMULATIONS

The basic numerical procedure employed in DD simulation is the solution of the equations of motion by an explicit central difference formula. In plasma simulations, it is common to employ the leapfrog method of solution which involves the evaluation of the momentum and position equations at different times instead of at the same time, as is standard for MD simulations [21]. The advantage of this method is that stable solutions are guaranteed with a suitable choice of timestep [22]. We will, however, use an explicit integration scheme with multiple time scales appropriate to the problem. Engquist and Hou [23] have recently shown that average difference approximations to partial differential equations can result in suppression of important oscillatory solutions because of gridding limitations. Explicit particle methods are therefore preferred. Initial sampling and ergodic mixing result in error cancellation in the explicit integration particle scheme [24]. In addition, implicit integration schemes for a large number of equations can be more computationally intensive.

If the timesteps chosen for the advancement of one dislocation with respect to another is too large, the dislocations can pass over each other in a given timestep. This is not favorable for simulating dislocation motion because if one of these dislocations is locked, the approaching dislocation (of the same Burgers vector) will in reality slow down as it comes in closer. If it is of the opposite Burgers vector, it will either annihilate or form a dipole.

The timestep chosen for the system must therefore be limited to the minimum amount of time it would take two dislocations to experience a reaction, whether it be collision or annihilation. If we consider two dislocations of arbitrary Burgers vectors coming in close vicinity to one another, this timestep can be expressed by the following condition:

$$\Delta t = \min \left( \frac{\Delta r_{ij}}{\Delta v_{ij}} \right) , \quad (12)$$

where  $\Delta r_{ij} = |r_i - r_j|$  and  $\Delta v_{ij} = |v_i - v_j|$ .

The consequence of this criterion is extremely crucial to the practical execution of a DD simulation. The reason for this is that the computation of the entire system may be unavoidably determined by the interaction of the two closest dislocations. This consequence is the potentially unnecessary reduction of the global timestep, and hence the escalation of computer costs due to the necessity of running for a longer time to achieve a practical simulation. Of course the reduction in timestep is necessary for limiting the first encounter of two dislocations, but what happens after that encounter is significantly more important in the determination of the ensuing timestep.

If the interacting dislocations which determine the timestep are approaching a stable configuration, then the timestep may be permanently determined by those two dislocations for the duration of the simulation. Once dislocations are immobilized however, they are no longer necessary for the determination of the simulation timescale simulation. Therefore, these dislocations may be tagged and decoupled from the calculation of the timestep but they still participate in the determination of the forces.

Simulation of a large number of dislocations would produce a distribution of dislocations in which the density of dislocations decreases farther away from the obstacle against which the dislocations are piling up. It is observed in experiments [25] that a pileup of no more than 50 to 100 dislocations actually occurs in one dimension. If the dislocations are placed uniformly on a line and a stress is applied in the direction of an obstacle, the group of dislocations will undergo a dynamic compression. Our results are shown in figure 2 for 50 dislocations. As time proceeds, the pileup shows a progressive concentration of dislocations toward the obstacle, as is expected from the physics. Comparisons between the results of the dynamic simulation of 100 dislocations against an obstacle show good agreement with analytical solutions for the equilibrium distribution [26].

Figure 3 shows the evolution of the trajectories of the first 7 dislocations from the same 50-dislocation pileup. It is seen in figure 3, however, that the leading dislocation reaches equilibrium early in the simulation. It would be practical to de-couple this dislocation from the overall calculation, as is done in MD [27]. It is found that a dislocation equilibrium position is achieved after 30 to 40 oscillations. A computational criterion of 30 to 40 oscillations is used to immobilize the dislocation. The immobilization technique gives an order of magnitude reduction in computing time without loss of accuracy.

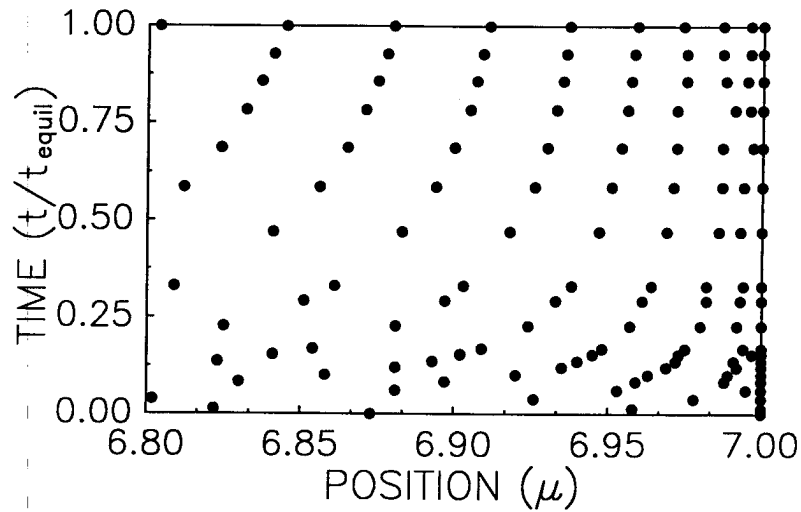


Figure 2. Time evolution of a 1-D 50-dislocation pileup.

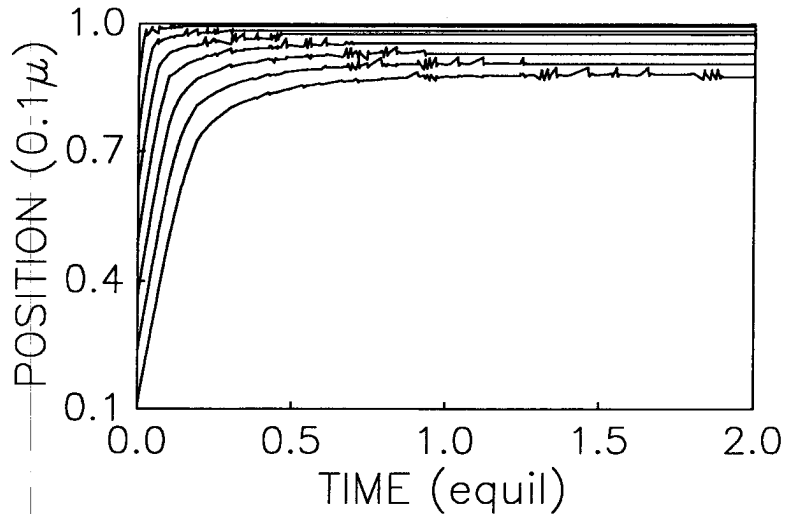


Figure 3. Spatial trajectories of the leading 7 dislocations in a 50-dislocation pileup (immobilization technique).

#### 4. TWO-DIMENSIONAL SIMULATIONS

A computer code, DISLOCAL, is being developed for the dynamic simulation of mobile dislocations. DISLOCAL also keeps track of short-range dislocation reactions. Separate vectors are assigned for the positions of immobile dislocations, dislocation dipoles, attractive junctions, clusters, and precipitate obstacles. Only mobile dislocations have additional velocity vectors.

At each timestep, the forces due to all obstacles upon each mobile dislocation are summed up. If two dislocations are close enough to form a dipole or

an obstacle, or annihilate, these dislocations are tagged and decoupled from the ensuing timestep calculation. Once all of the dislocation reactions have been compiled, the timestep criterion [equation (12)] is invoked upon all remaining mobile dislocations, and dislocations which have undergone reactions are removed from the mobile dislocation pool.

An additional constraint on the timestep criterion is that if two dislocations are causing a reduction in timestep over a significant period of time, these dislocations are removed from the mobile pool and the timestep is reset. This method of dynamic timestepping ensures that dislocation reactions do not significantly control the overall dynamics of the system.

Immobilization is a process included in the 2-D description in which mobile dislocations, which are nearly at equilibrium, are fixed and added to an immobile dislocation pool. The criterion for determining sufficient stability for immobilization is based upon the results for the 1-D simulation. Therefore, mobile dislocations for which a change of velocity vector is detected are observed for glide motion in opposite directions. If the total number of changes in direction is large within 40 timesteps, the dislocation is immobilized.

Savings in the total computational time (CPU and storage I/O requests) can be achieved by using the multiple timestep (MTS) method [28]. In this method, we represent the total force on a dislocation,  $i$ , as the sum of two components: a primary component ( $P_i$ ) and a secondary component ( $S_i$ ). The total force is given as the linear sum of the two, thus

$$F_{\text{tot}}^{(i)} = P_i + S_i \quad (13)$$

The primary force is taken as that resulting from dislocations within a short distance from the reference dislocation. The number of dislocations in this primary region is variable; however, force computations are performed every timestep. Beyond this primary region, the aggregate force due to all other dislocations is calculated at a lower frequency than every timestep. During intervening timesteps, the secondary force can be estimated by a Taylor series expansion:

$$S_i(t + m\Delta t) = S_i(t) + \dot{S}_i(t)m\Delta t + \frac{\ddot{S}_i(t)(m\Delta t)^2}{2!} + \dots \quad (14)$$

Results of dislocation simulations, considering only the long-range elastic field, indicate that the multiple timestep is beneficial when the total number of dislocations is large and when the number of dislocations in the primary region is a small fraction of the total.

Figure 4 shows the CPU time in the MTS method relative to direct calculations as a function of the fraction of dislocations in the primary region. The simulation contained 1000 dislocations. Also, the average relative error in force calculations is shown in the same figure. It is shown that the extra computations associated with the secondary force outweigh the benefit gained from the MTS method when the number of dislocations in the primary region exceeds 100. An optimal number of 40 results in an error on the order of 10% in force calculations.



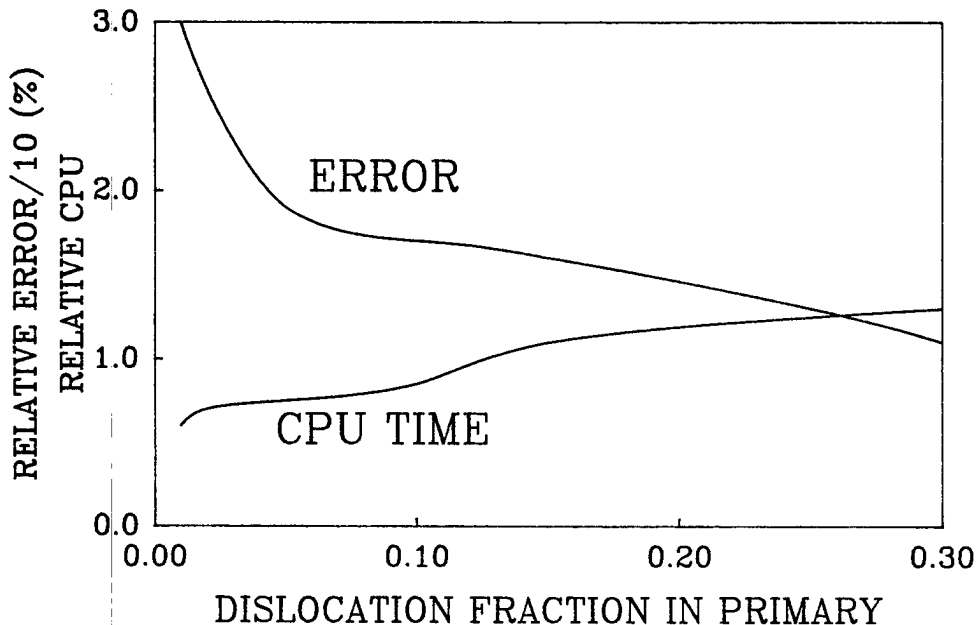


Figure 4. Relative error and CPU time as functions of the fraction of dislocations in the primary region.

Results of a simulation of this type are summarized in figure 5, which is a pictorial representation of a simulation of 50 dislocations over 50 timesteps. It is seen that dislocations are initially distributed over the entire grain. Dislocations are designated by the standard upside down "t" symbol,  $\perp$ , which identifies the direction of the dislocation and the Burgers vector. After a few timesteps, two dislocations near the top center of figure 5 satisfy the dipole formation criterion, and are fixed in space as a solid line on the figure. The symbol "x" is used to mark the dislocation which controls the global timestep calculations in each timeframe.

After more time has passed, dislocations which are attractive but not of opposite sign, form junctions (designated by  $\square$ ). These dislocations are removed from the mobile pool and deposited in an obstacle pool of dislocations. Three such attractive junctions form, and after each one forms the timestep which previously decreased in value due to junction interactions is increased over the subsequent iteration (figure 6). This is an example of dynamic time-stepping, and its effect on the simulation is that non-linear reactions are removed from the system over a short number of timesteps. The simulation indicates that clustering is a process which will ultimately lead to a more efficient use of computer time once it begins to occur.

##### 5. CONCLUSIONS

Dislocation dynamics simulation can be achieved by particle methods. Unique features of DD are the long-range nature of the elastic interaction field and the strong non-linear short-range dislocation reactions. The long-range field, which is vector and not scalar, results in  $O(n^2)$  computational complexity, where  $n$  is the number of dislocations.

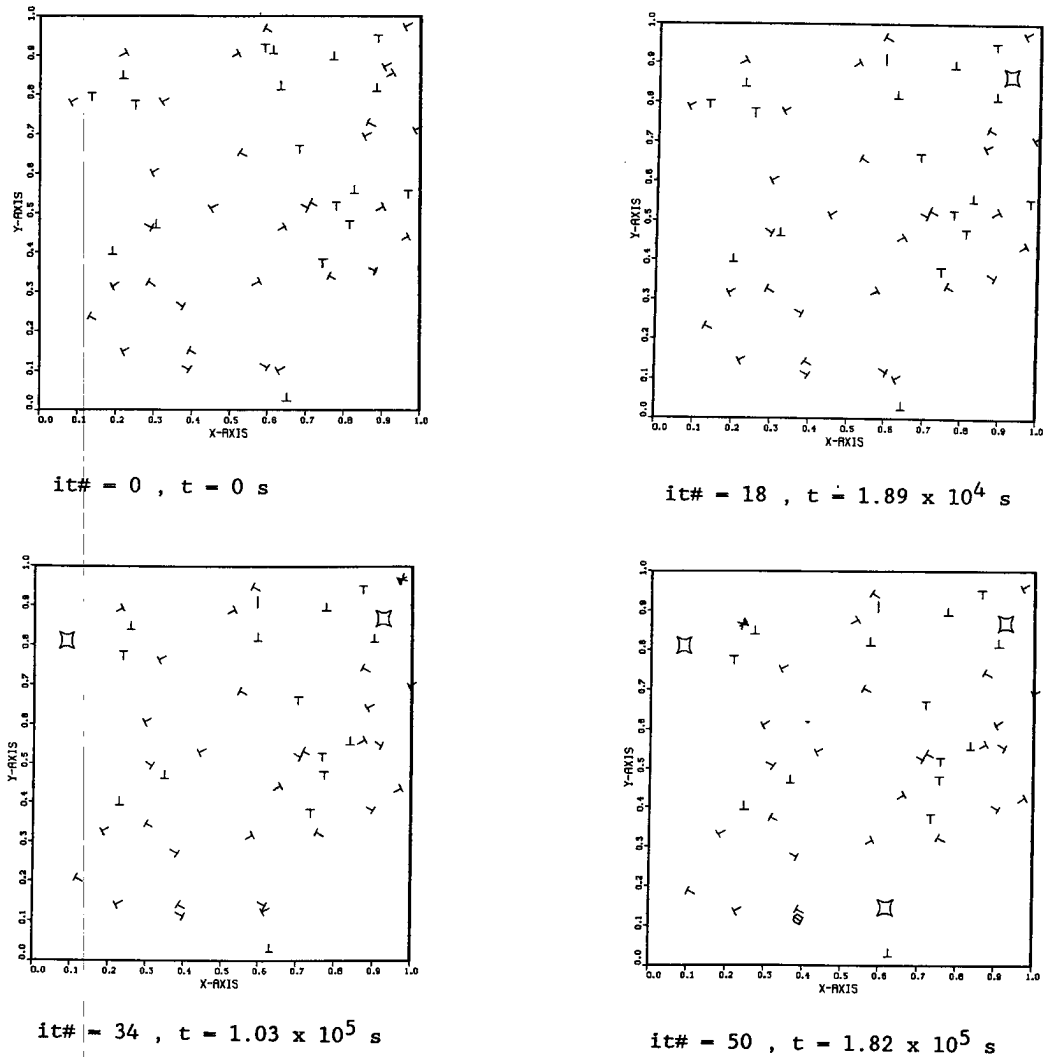


Figure 5. Two-dimensional dislocation simulation sequence.

Two methods which reduce this computational complexity have been applied in this work. First, the MTS method results in overall savings in computer time. Second, once clustering reactions start to occur, the order of computational complexity is reduced. In 1-D simulations of dislocation pileup, explicit integration of the EOM is shown to preserve spatial oscillations and is therefore preferred over implicit integration schemes. The evolution of the dislocation distribution function for the 1-D pileup shows small amplitude density fluctuations during the compression phase of the pileup.

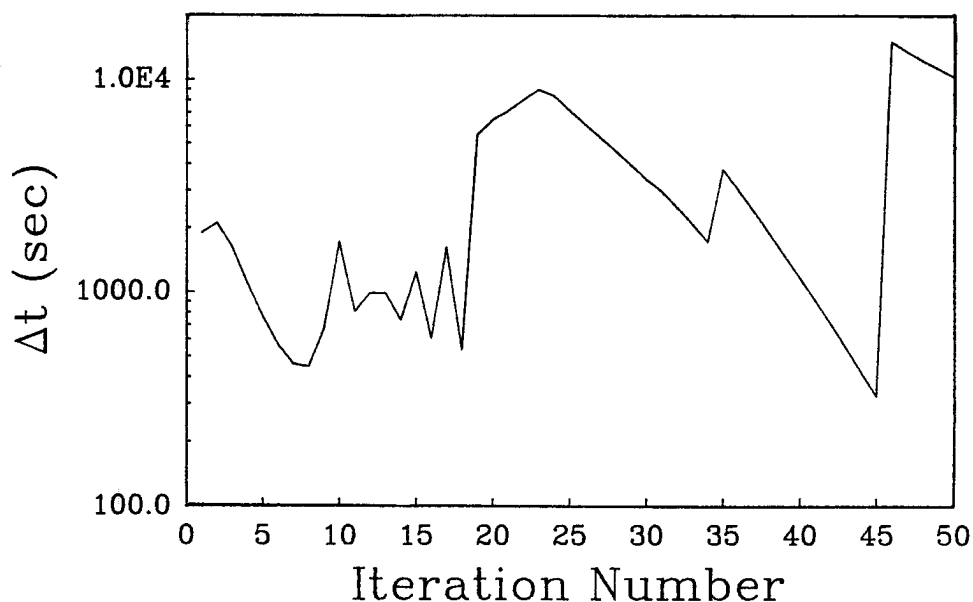


Figure. 6. Dependence of the dynamic timestep,  $\Delta t$ , on the simulation time.

#### ACKNOWLEDGEMENT

The work was supported by the U. S. Department of Energy, Office of Fusion Energy, Grant # DE-FG03-84ER52110, with UCLA.

#### REFERENCES

- 1) Abraham, F. F.: *Adv. Phys.*, 1986, 35, 1
- 2) Nicolis, G. and Prigogine, I.: *Self-Organization in Non-Equilibrium Systems* (Wiley, NY, 1977)
- 3) Walgraef, D. and Aifantis, E. C.: *Int. J. Engng. Sci.*, 1986, 24, 1789
- 4) Tabata, T., Fujita, H., Hiraoka, M., and Onishi, K.: *Philos. Mag.*, 1983, A47, 841
- 5) Mughrabi, H.: *Acta Metall.*, 1983, 31, 1367
- 6) Grosskreutz, J. C. and Mughrabi, H. in: *Constitutive Equations in Plasticity*, Ed. A. S. Argon (MIT Press, Cambridge, 1975) p. 251
- 7) Holt, D.: *J. Appl. Phys.*, 1970, 41, 3197
- 8) Argon, A. S. and Takeuchi, S.: *Acta Metall.*, 1981, 29, 1877
- 9) Sandstrom, R.: *Acta Metall.*, 1977, 25, 905
- 10) Walgraef, D. and Aifantis, E. C.: *Int. J. Engng. Sci.*, 1985, 23, 1351-1372
- 11) Schiller, C. and Walgraef, D.: "Numerical Simulations of Persistent Slip-Band Formation," *Acta Metall.*, 1987, to appear
- 12) Murphy, S. M.: "Spatial Instability in Dislocation Structure Under Irradiation," Theoretical Physics Division, AERE Harwell Report HL86/1383 (1986)
- 13) Hockney, R. W. and Eastwood, J. W.: *Computer Simulation Using Particles* (McGraw Hill, NY, 1981)
- 14) Andersen, H. C.: *J. Chem. Phys.*, 1980, 72, 2384
- 15) Peach, M. and Kohler, J. S.: *Phys. Rev.*, 1950, 80, 436
- 16) Takeuchi, S. and Argon, A. S.: *J. Mater. Sci.*, 1976, 11, 1542
- 17) Argon, A. S. and W. C. Mofatt, W. C.: *Acta Metall.*, 1981, 29, 293
- 18) Burton, B.: *Philos. Mag.*, 1985, A51, L13
- 19) Nabarro, F. R. N.: *Adv. Phys.*, 1952, 1, 271

- 
- 20) Essmann, U. and Mughrabi, H.: *Philos. Mag.*, 1979, 40, 731
  - 21) Verlet, L.: *Phys. Rev.*, 1967, 15, 98
  - 22) Birdsall, C. K. and Langdon, A. B.: *Plasma Physics via Computer Simulation* (McGraw Hill, NY, 1985)
  - 23) Engquist, B. and Hou, Y.: "Particle Method Approximation of Oscillatory Solution to Hyperbolic Differential Equations," to appear
  - 24) Neiderreither, H.: *Bull. Amer. Math. Soc.*, 1978, 84, 957
  - 25) Whelan, M. J., Hirsch, P. B., Horne, R. W., and Bollmann, W.: *Proc. Roy. Soc.*, 1957, A24, 524
  - 26) Amodeo, R. J. and Ghoniem, N. M.: "Dynamical Computer Simulation of the Evolution of a One-Dimensional Dislocation Pileup," *Int. J. of Eng. Sci.*, 1987, submitted
  - 27) Finnis, M. W. and Harker, A. H.: "A Users Guide to MOLDY, a Molecular Dynamics Program," AERE, Harwell Report AERE-R 8824 (1983).
  - 28) Swindoll, R. D. and Haile, J. M.: *J. Comput. Phys.*, 1984, 53, 289